

This is the peer reviewed version of the following article: Zhu, R, Guilbert, É, Wong, MS. Object-oriented tracking of thematic and spatial behaviors of urban heat islands. *Transactions in GIS*. 2020; 24: 85– 103, which has been published in final form at <https://doi.org/10.1111/tgis.12586>. This article may be used for non-commercial purposes in accordance with Wiley Terms and Conditions for Use of Self-Archived Versions. This article may not be enhanced, enriched or otherwise transformed into a derivative work, without express permission from Wiley or by statutory rights under applicable legislation. Copyright notices must not be removed, obscured or modified.

Object-oriented tracking of thematic and spatial behaviors of urban heat islands

Rui Zhu^{a,b}, Éric Guilbert^c, Man Sing Wong^{b,d,*}

^a*Senseable City Laboratory, Singapore-MIT Alliance for Research and Technology, Singapore*

^b*Department of Land Surveying and Geo-informatics, The Hong Kong Polytechnic University, Hong Kong, China*

^c*Department of Geomatics Sciences, Laval University, Québec, Canada*

^d*Research Institute for Sustainable Urban Development, The Hong Kong Polytechnic University, Hong Kong*

Abstract

Modeling thematic and spatial dynamic behaviors of Urban Heat Islands (UHIs) over time is important for understanding the evolution of this phenomenon to mitigate the warming effect in urban areas. Although previous studies conceptualized that a UHI only has a single life-cycle with spatial behaviors, a UHI can be detected to appear and to disappear several times periodically in terms of thematic and spatial integrated behaviors. Such multiple behaviors have not been illustrated with proof or evidence yet. This study conceptualizes a UHI as an object which has thematic and spatial behaviors simultaneously and proposes several graphs to depict periodic life-cycle transitions triggered by behaviors. The model has been implemented in an object-relational database management system and temperature readings collected numerous weather stations were interpolated as temperature images per hour. The results of this study indicate that the model could track the spatial and thematic evolution of UHIs continuously and reveal their periodical patterns and abnormal cases.

Keywords: Spatiotemporal data modeling; Object-oriented modeling; Urban heat islands

1. Introduction

An urban heat island (UHI) is an environmental phenomenon that air/land surface temperatures in urban areas are higher than that in surrounding rural areas. The existence of UHIs is a major problem in most metropolitan areas. They cause many adverse effects such as public health deterioration (Ding *et al.*, 2015; Kenney *et al.*, 2014; Morabito *et al.*, 2012), public security threats (Cohn and Rotton, 2000; Field, 1992; Rotton and Cohn, 2004), and increasing energy consumption (Fung *et al.*, 2006; Papakostas *et al.*, 2010). It is even a more serious problem in rapidly expanding cities given that the urbanization process is increasingly fast. An investigation into the adverse effects and exploring the causative factors of the phenomenon becomes urgent. Thus, it is needed to track evolutions of UHIs continuously in both thematic (i.e. temperature variations) and spatial (i.e. areal changes and topological transformations) dimensions over a long period.

Previous studies estimated land surface temperature (LST) in describing UHIs and analyzed its correlation with social indicators (Buyantuyev and Wu, 2010), environmental indices (Hu and Brunsell, 2015) and building impacts (Yuan and Ng, 2012; Wong and Nichol, 2013; Toparlar *et al.*, 2015; Wong *et al.*, 2016). Recent studies tend to analyze discrete pixels toward clustering UHIs as interactive objects extracted from thermal images. For example, object-based analysis clustered pixels of thermal infrared images as polygons of objects so that a strong correlation between spatial and thermal attributes (i.e. areal extent and LST) was revealed (Keramitsoglou *et al.*, 2011). However, these studies are incapable to track thematic and spatial changes of UHIs simultaneously over a long period. Although some empirical studies have been conducted by analyzing spatio-temporal variation patterns of UHIs based on the interpolation of air temperatures collected from meteorological

*Corresponding author

Email address: ls.charles@polyu.edu.hk (Man Sing Wong)

22 stations (Wu *et al.*, 2012; Kourtidis *et al.*, 2015), it is a challenge to describe instant changes at a
23 fine temporal resolution over a long time period. Thus, a model using spatio-temporal data is needed
24 for determining pixels of thermal images as UHI objects and tracking the changes of their dynamics
25 through continuous time.

26 Many studies of modeling geographical phenomena as field objects have included variable bound-
27 aries determined by other properties (e.g. temporal and thematic properties) related to the field
28 (Goodchild *et al.*, 2007). Their dynamics could be represented in a hierarchical framework where a *se-*
29 *quence* was composed of consecutive *zones* and related together in *processes*, and *events* for observing
30 their shape changes and spatial movements from a series of images (McIntosh and Yuan, 2005; Yuan
31 and Hornsby, 2008). For instance, moving behaviors of each object were modeled as a set of semantic
32 *events* such as *departure* and *arrival* and patterns were constructed from several sequences of the
33 *events* (Hornsby and Cole, 2007). Other developed models conceptualized spatiotemporal dynamic
34 phenomena as geo-entities in relationships and implemented data structures fitted for computations
35 (Bothwell and Yuan, 2010; Pultar *et al.*, 2010; Li *et al.*, 2013). These approaches provide an appro-
36 priate strategy to model the dynamics of UHIs. For example, a series of zones of UHIs which expand
37 continuously can correspond to a sequence.

38 However, UHI evolutions may involve a single object or several different objects that associate
39 with topological relationships between zones of UHIs. For example, a UHI can contract, split into two
40 parts and disappear. Oppositely, two UHIs can expand and merge into one. Claramunt and Thériault
41 (1995) proposed a series of the topological process describing the behavior of a single object as an
42 expansion or a contraction and behaviors between several objects as splits, unions, or re-allocations.
43 Similar models were developed as such that objects disappear and reappear because of merging and
44 splitting behaviors (Renolen, 2000; Nixon and Hornsby, 2010; Bothwell and Yuan, 2011). These
45 studies provide an enlightening approach for modeling complex transformation of UHIs. However,
46 they only focused on conceptual modeling and tracking UHIs needs logistical modeling incorporated
47 into systematically conceptualized UHI behaviors. Furthermore, Del Mondo *et al.* (2013) depicted
48 topological transformations in a *graph* composed of a set of nodes and several edges connecting the
49 nodes with certain filiation relationships. Similarly, different graphs will be proposed to develop
50 tracking dynamics of UHIs in our study.

51 A study has already proposed an object-oriented spatio-temporal framework in modeling the spatial
52 behavior of UHIs (Zhu *et al.*, 2017a). Within this framework, a UHI was defined as a two-dimensional
53 field object whose temperatures were equal to or higher than a reference rural temperature. A UHI may
54 experience different sequences, each of which corresponds to a type of spatial behavior. The changes
55 of UHI can be either internal with area changes or external involving topological transformations with
56 one or several UHIs. In addition, spatial behaviors have been defined into two graphs; namely, a zone
57 graph $\mathcal{G}_Z = (\mathcal{Z}, \mathcal{F}_z)$ which denotes a set of zones (\mathcal{Z}) as nodes and a set of filiations (\mathcal{F}_z) as edges
58 (e.g., spatial behaviors of zones) associated with the zones; and a sequence graph $\mathcal{G}_S = (\mathcal{S}, \mathcal{E}_s)$ which
59 represents a set of sequences (\mathcal{S}) that cover area changes or topological transformations (\mathcal{E}_s).

60 However, the aforementioned framework is lacking the capability to investigate temperature vari-
61 ations in the UHI extent, since the field was conceptualized and recorded as a homogeneous surface.
62 Temperature distribution in a real situation within the UHI extent can vary significantly. For example,
63 the temperature of a small area within a UHI may be steady, whereas the temperature of other areas
64 in the same UHI may go up corresponding to a place with accumulated anthropogenic heat. The UHI
65 may be considered as consisting of several small UHIs if the small areas are reckoned as UHIs with
66 higher intensity. To have a better investigation into this phenomenon at different thematic intensities,
67 a new definition of UHI will be introduced.

68 It was suggested that geographical phenomena may have a periodical process of state transitions

69 between existence and non-existence (Hornsby and Egenhofer, 2000). As an object, a UHI may appear,
70 disappear and reappear over time. In this consideration, the periodicity links a series of existences
71 as a continuous process, in which the life span of UHIs can extend from a few hours to a couple of
72 days. Thus, establishing the periodicity of UHIs for the investigation over long periods becomes very
73 important for our study.

74 In addition, the above framework cannot track thematic changes of a UHI. This point is vital to
75 clarify evolutionary trends of temperatures since they determine the spatial extent conclusively and
76 influence its spatial behaviors consequently (Bothwell and Yuan, 2012). For example, an increase of the
77 UHI temperature may lead to the expansion of its spatial extent at night-time but contraction during
78 the daytime. Therefore, thematic tracking will also be modeled in our study to explore thematic-
79 associated spatial behaviors.

80 To build a relationship between two zones at two consecutive time instants for computing the
81 proposed spatial behaviors, the above framework only covered the relationship between the overlapping
82 area and the zone in the prior time instant. This may cause a problem that two zones having no
83 significant overlapping with each other are still determined as associated zones uncertainly, but UHI
84 is a localized phenomenon having no significant displacement (Hua and Wang, 2012; Jalan and Sharma,
85 2014). To solve this problem, a refined method is also necessary.

86 In summary, this study has four originalities: (i) a new concept of UHI will be presented in
87 considering of difference between urban and rural air temperatures; (ii) periodical process of UHIs
88 with state transitions will be proposed to allow UHIs to have longer life spans; (iii) thematic behaviors
89 as well as UHI graphs will be proposed and modeled to track the changes in a variety of aspects; and
90 (iv) a refined and robust computational method will be developed.

91 The rest paper is organized into three sections. Section 2 presents a new conceptual model of
92 UHIs viewed as dynamic objects and emphasizes on spatial and thematic behaviors with periodical
93 transitions. Section 3, through an empirical evaluation in a developed spatial database management
94 system, suggests the effectiveness of the proposed model. Finally, Section 4 draws the discussion and
95 conclusion of this study.

96 2. Conceptual and logical modeling

97 2.1. UHIs as dynamic objects

98 During its lifetime, a UHI evolves through different stages. As shown in Figure 1, a UHI occurs
99 at a given time and place if the temperature measured at this location is higher than a reference
100 rural temperature. The *intensity* at a point is defined by this temperature difference (d). The UHI is
101 characterized when the temperature difference is above a certain threshold, the *magnitude*.

102 As a temporal phenomenon, a UHI may expand, contract, or remain stable possibly because the
103 intensity grows up, drops down, or remains constant over time. This variation in the extent and
104 intensity of the UHI describes its behavior and can be summarized by a series of concepts represented
105 in Figure 2. The behavior can describe a continuous process or a transformation. Continuous processes
106 can be spatial (when they describe a variation of the UHI extent) or thematic (a variation of intensity).

107 UHIs also show periodical behavior. Since temperature varies periodically, with for example UHI
108 episodes more intense at night or during the summer, UHI should be allowed to disappear and reap-
109 pear periodically at the same location. This consideration is helpful to reveal thematic and spatial
110 evolutionary trends of UHIs over longer periods (e.g., in months, seasons, or even years). In this
111 regard, a UHI can go through several *active* and *inactive* periods (Figure 3). In this scenario, the
112 *appearance* of a UHI indicates a *creation* if it is newly generated and *activation* if it existed before,
113 and *disappearance* may lead to *death* if it disappears forever.

114 An active period can start from behaviors when zones appear and terminate at behaviors when
 115 zones disappear. However, termination of an *active period* followed by an *inactive period* means that
 116 the UHI is disappeared temporarily and it will appear again shortly. Therefore, this process requires
 117 some topological constraints:

- 118 • disappeared zones which will be activated cannot be made by *annexation* and *merging* since
 119 disappeared zones associated with the two behaviors are destructed forever; and
- 120 • activated zones which 118 have been created cannot come from *separation* and *splitting* because
 121 both behaviors generate entirely new objects.

122 2.2. Graph-based modeling of UHI behaviors

123 UHIs are observed from temperature data at given timestamps. At a timestamp t_i , a UHI u_n is
 124 observed by a zone z_n^i where the temperature is above the magnitude. A UHI will have a lifespan
 125 starting at t_i , when its first occurrence z_n^i is observed and ending at t_n^j when its last occurrence is
 126 observed. In between, the UHI goes through active and inactive periods and, in each active period,
 127 it goes through different sequences characterized by the behaviors of Figure 2. Hence, as [Zhu et al.](#)
 128 (2017a), sequences are defined by a series of zones and relationships between zones and sequences
 129 are defined by a graph. Furthermore, we add one level since a series of sequences form a period. In
 130 addition, we consider temperature to define trends in intensity variation.

131 In order to detect all behaviors, it firstly needs to have the set of all zones identified at all times-
 132 tamps \mathcal{Z} . A sequence s_n^i is then a series of consecutive zones following the same spatial behavior. As
 133 [Zhu et al. \(2017a\)](#) proposed, two graphs are built to define the spatial behavior. The zone graph is
 134 noted $\mathcal{G}_Z = (\mathcal{Z}, \mathcal{F}_z)$ where (\mathcal{F}_z) are edges connecting the zones and corresponding to some on-going
 135 process or transformation. The sequence graph $\mathcal{G}_S = (\mathcal{S}, \mathcal{E}_s)$ represents a set of sequences (\mathcal{S}) that
 136 have areal changes or topological transformations defining the set of edges (\mathcal{E}_s) of \mathcal{G}_S .

137 Similarly, we define a graph storing variations in trends of intensity. The intensity of a UHI can
 138 increase, decrease or remain stationary. A *chain* is defined as a series of zones where the intensity
 139 evolves according to a constant trend (Figure 3). Hence, a *chain* can be noted $c_n = \{z_n^i, \dots, z_n^j\}$
 140 where for any k in $[i + 1, j]$, variations between $I(z_n^{k-1})$ and $I(z_n^k)$ are of the same kind, where $I(z)$
 141 is the intensity of zone z , equaling to the mean value of the temperature differences. Thus, a new
 142 graph of chains is introduced: $\mathcal{G}_C = (\mathcal{C}, \mathcal{F}_C)$ where \mathcal{C} is the set of chains and \mathcal{F}_C the filiations between
 143 consecutive chains. As with periods, transitions between chains can be defined by:

- 144 • if $c_n^{i_{j-1}}$ increases and $c_n^{i_j}$ decreases, u_n reaches a *peak* at the transition;
- 145 • if $c_n^{i_{j-1}}$ decreases and $c_n^{i_j}$ increases, u_n reaches a *low* at the transition;
- 146 • if $c_n^{i_{j-1}}$, $c_n^{i_j}$, and $c_n^{i_{j+1}}$ respectively increases, stays stationary and decreases, chain $c_n^{i_j}$ corresponds
 147 to a plateau. u_n is *reaching a plateau* and *leaving a plateau* during the transitions;
- 148 • if $c_n^{i_{j-1}}$ decreases, $c_n^{i_j}$ keeps stationary, and $c_n^{i_{j+1}}$ increases, chain $c_n^{i_j}$ is as a floor. u_n is *reaching*
 149 *a floor* and *leaving a floor* during the transitions; and
- 150 • if both $c_n^{i_{j-1}}$ and $c_n^{i_{j+1}}$ increase or decrease and $c_n^{i_j}$ is stationary, chain $c_n^{i_j}$ represents a pause for
 151 the thematic evolution. The two consecutive transitions are *stabilization* and *resumption*.

152 A series of consecutive sequences or chains starting with an appearance and a disappearance form
 153 an *active period*. Similarly, an *inactive period* contains an empty sequence and is denoted as p_n^b so that
 154 an *awakened* connects with an empty sequence and generates another practical sequence. Thereby,
 155 all the periods can be refined into a graph $\mathcal{G}_P = (\mathcal{P}, \mathcal{E}_p)$ where \mathcal{P} is the set of nodes denoting periods
 156 and \mathcal{E}_p is the set of edges representing the state transitions between the periods. When several UHIs

157 have interactive evolution in the same urban area or spatial contiguous city clusters, a graph can be
 158 introduced as $\mathcal{G}_U = (\mathcal{U}, \mathcal{E}_u)$, where \mathcal{U} is a set of UHIs that makes the graph nodes and \mathcal{E}_u is the edges
 159 composed by topological transformations which lead the creation and destruction of the UHIs. In
 160 summary, three hierarchical graphs have been proposed (Figure 4). Thematic filiations construct the
 161 chain-graph \mathcal{G}_C . \mathcal{G}_P records complete life-cycle of a UHI which may have several consecutive periods
 162 associated with some particular transformations. Ultimately, all of the UHIs evolution can be finally
 163 tracked in \mathcal{G}_U .

164 2.3. Extraction of UHI changes

165 The change of a UHI was built up by studying overlapping zones at consecutive time instants. If
 166 two zones share a similar position, they are most likely belonging to the same UHI. Let z^i and z^{i-1}
 167 be two zones at consecutive time instants t_i and t_{i-1} . Two irrelevant zones may be associated if only
 168 considering the relation between the intersection $z^i \cap z^{i-1}$ and z^{i-1} , because UHIs remain at the same
 169 location and do not have significant displacements. Thus, it is more convincing if related zones have
 170 a significant intersection $z^i \cap z^{i-1}$ for both z^i and z^{i-1} .

171 Given two zones z and z' , we consider that z significantly overlaps z' and we note it $SO(z, z')$ if
 172 both zones overlap and the area of their intersection is large enough concerning the area of z' . If we
 173 note $0 < \varepsilon < \frac{1}{2}$ being a constant, significant overlap is defined by:

$$SO(z, z') \Leftrightarrow \frac{\text{area}(z \cap z')}{\text{area}(z')} > 1 - \varepsilon \quad (1)$$

174 Fixing $\varepsilon < \frac{1}{2}$ guaranties that for a given zone z' , it is not possible to find two disjoint zones
 175 significantly overlapping z' . This relation is not symmetric and the relation $SO(z', z)$ may be false, if
 176 z is much larger than z' . If both relations are true, both zones significantly overlap and we note this
 177 relation $OO(z, z')$ as

$$OO(z, z') \Leftrightarrow SO(z, z') \wedge SO(z', z) \quad (2)$$

178 Although a zone cannot be significantly overlapped by two disjoint zones, it can significantly
 179 overlap several zones. For a given set of zones Z , the set of all zones significantly overlapped by z is
 180 given by

$$S_Z(z) = \{SO(z, z') | z' \in Z\} \quad (3)$$

181 For a given zone z , the number of zones in $S_Z(z)$ is given by $\#S_Z(z)$. If Z is the set of all zones \mathcal{Z}_i
 182 at time i , we simply note $S_{\mathcal{Z}_i}$ as S^i and its cardinality $\#S^i$. As zones at a given time instant are
 183 supposed to be disjoint, we have

$$z \in \mathcal{Z}_i, z' \in \mathcal{Z}_i \Rightarrow z \cap z' = \emptyset \quad (4)$$

184

$$z_1^i \in \mathcal{Z}_i, z_2^i \in \mathcal{Z}_i, z^j \in \mathcal{Z}_j \Rightarrow \neg (SO(z_1^i, z^j) \wedge SO(z_2^i, z^j)) \quad (5)$$

185 The type of spatial behavior of a UHI can be determined by the number of zones with which it
 186 is associated by the type of filiation with these zones. The UHI has (i) area change if it associates
 187 with only one zone and without any topological transformations, (ii) appearance or disappearance
 188 if no overlapping or no association occurs, or (iii) transformations when overlapping and associating
 189 with several other zones. Thus, spatial behaviors can be conceptualized as *expansion*, *continuation*,
 190 and *contraction* if z^i significantly overlaps one zone at t_{i-1} , and the area of z^i is larger, equivalent
 191 and smaller, respectively. In addition, z^i can have topological transformations as *appearance* if z^i has
 192 no significant overlap between any zones at t_{i-1} , and as *disappearance* if z^i has no significant overlap
 193 between any zones at t_{i+1} . The other two transformations may occur when more zones are associated:

- 194 • *merge*: z^i overlaps several zones at t_{i-1} and each overlapping area is significant to its corre-
195 sponding zone at t_{i-1} . If only one overlapping area is exclusively significant to the zone at t_i ,
196 the associated zone at t_{i-1} continues as z^i with an *annexation*. Otherwise, a *merging* happens;
- 197 • *split*: several zones at t_i overlap at z^{i-1} and each overlapping area is significant to its corre-
198 sponding zone at t_i . If area of z^{i-1} equals to one particular zone at t_i , a *separation* is derived.
199 Otherwise, a *splitting* occurs.

200 2.4. Modeling spatial behaviors

201 We now can redefine the transitions between zones from their relationships. If a UHI does not
202 undergo any transformation between time t_{i-1} and time t_i , then $\#S^i(z^{i-1})$ and $\#S^{i-1}(z^i)$ cannot be
203 greater than 1. If no change in an area occurs, both zones significantly overlap such that $OO(z^{i-1}, z^i)$
204 is true. Hence for two zones $z^{i-1} \in \mathcal{Z}_{i-1}$ and $z^i \in \mathcal{Z}_i$, continuation is defined by

$$\text{continuation}(z^{i-1}, z^i) \Leftrightarrow OO(z^{i-1}, z^i) \wedge \#S^i(z^{i-1}) = 1 \wedge \#S^{i-1}(z^i) = 1 \quad (6)$$

205 In a contraction, z^{i-1} is bigger than z^i hence only $SO(z^{i-1}, z^i)$ is true. As a continuous process,
206 no other zone is involved in the process. Therefore, the contraction is defined by

$$\text{contraction}(z^{i-1}, z^i) \Leftrightarrow SO(z^{i-1}, z^i) \wedge \#S^i(z^{i-1}) = 0 \wedge \#S^{i-1}(z^i) = 1 \quad (7)$$

207 Similarly, the expansion is defined by

$$\text{expansion}(z^{i-1}, z^i) \Leftrightarrow SO(z^i, z^{i-1}) \wedge \#S^i(z^{i-1}) = 1 \wedge \#S^{i-1}(z^i) = 0 \quad (8)$$

208 Referring to Figure 2, a process (more specifically for an area change) is a relationship involving
209 a limited number of zones. Anything that is not a process can then be defined as a transformation.
210 The above three relationships correspond to processes where no topological change occurs. A more
211 general relation can be defined relating two consecutive zones that are parts of a continuing process.

$$\text{process}(z^{i-1}, z^i) \Leftrightarrow (SO(z^{i-1}, z^i) \vee SO(z^i, z^{i-1})) \wedge \max(\#S^i(z^{i-1}), \#S^{i-1}(z^i)) = 1 \quad (9)$$

212 Transformations can involve several zones as different UHIs may be engaged. For example, a
213 merge involves a set of zones $Z = \{z_1^{i-1}, \dots, z_m^{i-1}\} \subset \mathcal{Z}_{i-1}$ and one zone $z^i \in \mathcal{Z}_i$. The zone z^i has to
214 significantly overlap all the zones of Z . On the opposite, no zone of \mathcal{Z}_{i-1} significantly overlaps z^i .

$$\text{merging}(Z, z^i) \Leftrightarrow (S^{i-1}(z^i)) \wedge (\forall z \in \mathcal{Z}_{i-1}, \neg SO(z, z^i)) \quad (10)$$

215 In the case where another zone $z_0^{i-1} \in \mathcal{Z}_{i-1}$ significantly overlaps z^i , we have an annexation instead
216 of a merge.

$$\text{annexation}(z_0^{i-1}, Z, z^i) \Leftrightarrow (S^{i-1}(z^i)) \wedge (\forall z \in Z, \neg SO(z, z^i)) \wedge SO(z_0^{i-1}, z^i) \quad (11)$$

217 The other way around, one zone z^{i-1} at t_{i-1} overlapping a set of zones $Z = \{z_1^i, \dots, z_m^i\} \subset \mathcal{Z}_i$
218 at t_i corresponds to a split. This requires that z^{i-1} significantly overlaps all the zones of Z while no
219 zone overlaps z^{i-1} significantly.

$$\text{splitting}(z^{i-1}, Z) \Leftrightarrow (S^i(z^{i-1})) \wedge (\forall z \in \mathcal{Z}_i, \neg SO(z, z^{i-1})) \quad (12)$$

220 Instead, a separation occurs if one zone z_0^i significantly overlaps z^{i-1} .

$$\text{separation}(z^{i-1}, Z, z_0^i) \Leftrightarrow (S^i(z^{i-1})) \wedge (\forall z \in Z, \neg SO(z, z^{i-1})) \wedge SO(z_0^i, z^{i-1}) \quad (13)$$

221 Finally, a zone $z^i \in \mathcal{Z}_i$ can appear or disappear at time t_i . In the first case, it is not related to
222 any zone in \mathcal{Z}_{i-1} , in the second case, it is not be related to any zone in \mathcal{Z}_{i+1} .

$$\text{appearance}(z^i) \Leftrightarrow \forall z \in \mathcal{Z}_{i-1}, \neg (SO(z, z^i) \vee SO(z^i, z)) \quad (14)$$

$$\text{disappearance}(z^i) \Leftrightarrow \forall z \in \mathcal{Z}_{i+1}, \neg (SO(z, z^i) \vee SO(z^i, z)) \quad (15)$$

224 Zones would have different spatial behaviors when their overlaps are in different scenarios. For
 225 example, if $SO(z_b, z_c)$ and $SO(z_b, z_a)$ are true, it's a merge. With a different epsilon $SO(z_b, z_c)$ and
 226 $SO(z_a, z_b)$, an annexation could be obtained (Figure 6). We may also have $SO(z_a, z_d)$, which leads
 227 to a split. In this case, z_a would have a special behavior, combining a split and a merge at the same
 228 time.

229 2.5. Modeling thematic behaviors

Studying thematic behaviors is done by measuring the evolution of intensity through time. From one instant to the next, it can *increase*, *decrease* or remain *stationary*. Indeed, if the intensity remains within a limited range, it reasonable to consider it is *stationary*.

$$\text{decrease}(z^{i-1}, z^i) \Leftrightarrow I(z^{i-1}) - I(z^i) > \varepsilon \quad (16)$$

$$\text{increase}(z^{i-1}, z^i) \Leftrightarrow I(z^i) - I(z^{i-1}) > \varepsilon \quad (17)$$

$$\text{stationary}(z^{i-1}, z^i) \Leftrightarrow |I(z^{i-1}) - I(z^i)| < \varepsilon \quad (18)$$

230 2.6. Modeling consecutive active-periods

231 Determination of two consecutive active periods connected by an inactive period is a necessity to
 232 construct a UHI. As conceptualized above, z^i could either derive a creation if it is newly generated
 233 or an activation if it has already existed. When z^i appears, a retrospective trace will check whether
 234 there was a disappeared z^{i-x} at the same location. Two active periods can be connected if (z^{i-x}, z^i)
 235 are spatially associated.

$$\text{consecutive}(p_n, p'_n) \Leftrightarrow (\text{process}(z^{i-x}, z^i) \wedge (x \geq 2)) \wedge (\neg \text{process}(z^{i-y}, z^i) \wedge (\forall y < x)) \quad (19)$$

236 3. Empirical evaluation

237 3.1. Study area and pre-processing

238 Guangzhou, located in the humid subtropical climate, is one of the most urbanized cities in China
 239 and has a population over 13 billion. It has high temperatures throughout the year. Since the model
 240 requires high temporal resolution of the data set to track changes of UHIs continuously, hourly updated
 241 near-surface (approximately 1.5 meters above land surface) air temperatures were measured in 216
 242 automatic weather stations (Figure 5), 159 of which were located in the urban area of 3660 km² in
 243 size. Major stations in urban areas were on concrete surfaces besides roads and/or buildings. To
 244 analyze evolutionary trends of UHIs over a long time, data were collected during a long time in the
 245 year 2015 with an interval of 21 days between every two weeks, from July 31 to August 6, August 28
 246 to September 3, September 25 to October 1, October 23 to October 29, November 20 to November
 247 26, and December 18 to December 24.

248 To obtain a series of temperature images from the weather stations, an interpolation method of
 249 Universal Kriging was used as the method can highlight “hotspot” regions of UHIs supposing the input
 250 data set which contains an overriding trend (Chai *et al.*, 2011; Hofstra *et al.*, 2008; Irmak *et al.*, 2010;
 251 Stahl *et al.*, 2006). Since weekly-averaged root mean square errors of the six sequential weeks were 1.06
 252 °C, 0.99 °C, 1.13 °C, 1.06 °C, 1.07 °C, and 1.03 °C, the magnitude m should be notably larger than
 253 1 °C to extract zones of UHIs confidently. Temperatures observed as the red star symbol in Figure 5
 254 were recorded in the Dajinfeng Eco-scenic Park which is a forestry area close to urban areas so they
 255 can represent as rural temperatures confidently to extract zones of UHIs and will not be affected by
 256 the heat dispersed from urban areas. Also, several other rural stations have lower temperatures so

SQL 1 FUNCTION ActivePeriod()

```
1 INSERT INTO period(pid, t_s, czid, pzid, spb, thb)
2 SELECT max(path) AS path, per.t_s, per.czid, per.pzid, per.spb, per.thb
3 FROM (WITH RECURSIVE per_u(path, t_s, czid, pzid, spb, thb)
4       AS (SELECT row_number() OVER (ORDER BY t_s) AS path, root.t_s,
5           root.czid, root.pzid, root.spb, root.thb
6       FROM behavior AS root UNION
7       SELECT leaf.path, root.t_s, root.czid, root.pzid, root.spb, root.thb
8       FROM behavior AS root, per_u AS leaf
9       WHERE root.czid = leaf.pzid
10      AND leaf.pzid > 0 AND leaf.spat_beh <> 'separa_d_obj'
11      AND root.spb <> 'annexa_d_obj'
12      AND root.spb <> 'merging' AND root.spat_beh <> 'splitting')
13 SELECT * FROM per_u ORDER BY path, t_s) AS per
14 GROUP BY per.t_s, per.czid, per.pzid, per.spb, per.thb;
```

257 that rural areas may be included as part of a UHI if these stations are used. Therefore, only one rural
258 station was used as the reference of rural temperatures to extract zones of UHIs.

259 3.2. System Implementation

260 The model has been implemented in PostgreSQL 10 to simulate behaviors and to track their
261 changes during the complete life-cycles of UHIs. A UML model is presented in Figure 7, which
262 summaries the classes as discrete records in tables and represents their associations. First, a time
263 series of temperature images generated hourly from air temperatures are compiled in a set of **image**
264 tables. Hence, all the zones are extracted from temperature images, and their spatial and thematic
265 information is tabulated in the **zone** table. For example, each row records a unique zone identified
266 by its ID (**zid**), which exists as a single polygon (**shape**) at a timestamp (**t_s**). Temperatures in
267 the **shape** are at least with a magnitude (**m**) higher than the reference rural temperature (**rural_t**).
268 Particularly, four types of thermal intensities are also summarized (**max_t**, **min_t**, **mea_t**, and **mod_t**).
269 In order to determine filiation relations between zones, overlapping areas (**overlap_area**) of zones at
270 the current instant (**czid**) and zones in the previous instant (**pzid**) should be calculated in advance.
271 To avoid duplicate calculation, zones with area changes and topological transformations are classified
272 into three tables (**merge**, **split**, and **area_change**) such that the **behavior** table can be built as the
273 central domain to describe two types of behaviors (**spb** and **thb**) at each timestamp (**t_s**). Thus,
274 UHIs (**oid**) can be constructed in the **uhi** table, and each UHI can have one or several periods
275 (**pid**), and each period combines a time serial of spatial behaviors determined by thematic behaviors.
276 Simultaneously, sequence and process descriptions for spatial behaviors (**spid**) and thematic behaviors
277 (**cid**) are obtained, and their corresponding patterns (**spp** and **thp**) are finally shown.

278 It is necessary to identify topological relations associated with zones that can create and destroy
279 an active period (SQL 1). It is also vital to connect active periods that belong to the same UHI by
280 determining awakened zones that trigger new periods (SQL 2). In SQL 1, lines 4-6 generate serial
281 numbers as candidates of period IDs and determine the first zone behavior (i.e. named as **root**) in the
282 periods. Lines 7-12 build continual zone behaviors that extend from the roots (i.e. named as **leaf**).
283 More specifically, line 9 connects the leaves to the root. Line 10 avoids endless loop computation by
284 ensuring that the appearance and disappearance behaviors are included in the period, and generates
285 new periods when zones are separated as different objects. Lines 11-12 cut off the extension of leaves
286 when zones are destroyed. Lastly, lines 3-13 execute the recursive computation and lines 2-14 select
287 the maximum value of path used as the final period ID. In SQL 2, lines 5-6 and 7-8 list zones having
288 *appearance* as the head and *disappearance* as the tail respectively, where time interval between them
289 is more than two hours but no longer than the maximum awakened time (lines 9-10). Thus, pairs

SQL 2 FUNCTION Awake(sleep_t, min_r, min_rein)

```
1 INSERT INTO awake(disappeared_zid, appeared_zid)
2 SELECT tail_seq.zid AS disap_z, head_seq.zid AS reapp_z,
3     (head_seq.t_s - tail_seq.t_s) AS dth_t,
4     ST_Area(ST_Intersection(head_seq.geom, tail_seq.geom)) AS i_a
5 FROM (SELECT zone.* FROM zone, period
6     WHERE spb = 'appearance' AND zone.zid = period.czid) AS head_seq,
7     (SELECT zone.* FROM zone, period
8     WHERE spb = 'disappearance' AND zone.zid = period.pzid) AS tail_seq
9 WHERE head_seq.t_s - tail_seq.t_s <= sleep_t * 3600 * '1 second'::INTERVAL
10 AND head_seq.t_s - tail_seq.t_s >= 2 * 3600 * '1 second'::INTERVAL
11 AND ST_Area(ST_Intersection(head_seq.geom, tail_seq.geom))/ST_Area(head_seq.geom) >= min_r
12 AND ST_Area(ST_Intersection(head_seq.geom, tail_seq.geom))/ST_Area(tail_seq.geom) >= min_r
13 AND ST_Area(ST_Intersection(head_seq.geom, tail_seq.geom))/ST_Area(head_seq.geom) >= min_rein;

14 INSERT INTO awake(disappeared_zid, appeared_zid)
15 SELECT cand.disap_z, cand.reapp_z
16 FROM awakened_cand AS cand,
17     (SELECT cand.reapp_z, min(cand.dth_t) AS min_dth_t
18     FROM awakened_cand AS cand,
19     (SELECT min(dth_t) AS min_dth_t, disap_z
20     FROM awakened_cand GROUP BY disap_z) AS dth_cand,
21     (SELECT max(i_a) AS max_i_a, dth_t, disap_z
22     FROM awakened_cand GROUP BY disap_z, dth_t) AS ints_cand
23     WHERE dth_cand.min_dth_t = cand.dth_t AND dth_cand.disap_z = cand.disap_z
24     AND ints_cand.max_i_a = cand.i_a AND ints_cand.disap_z = cand.disap_z
25     AND dth_cand.disap_z = ints_cand.disap_z GROUP BY cand.reapp_z) AS uhi_cand
26 WHERE cand.reapp_z = uhi_cand.reapp_z
27 AND cand.dth_t = uhi_cand.min_dth_t;
```

290 of the heads and tails that satisfy the awakened condition (lines 11-13) are selected as the awakened
291 candidates (lines 2-3). However, several disappeared zones can map to the same appeared zone in the
292 awakened candidates. On the basis of the candidates which have the minimum sleeping time (lines
293 19-20), zones having the maximum overlapping area are selected (lines 21-22) from the records of
294 awakened candidates (lines 23-25). Finally, zones satisfying all the conditions are inserted into the
295 awake table (lines 14-27).

296 3.3. Results

297 3.3.1. Dynamic behaviors of UHIs

298 Figure 8 presents seven consecutive days of the intensities (i.e. the mean value of temperature
299 differences at each time instant) in five different magnitudes. Intensities ($m = 1$ °C) lasting almost
300 all the time and suggesting that $m = 1$ °C cannot distinguish temperature difference effectively.
301 It proves that zones of UHIs should be with $m > 1$ °C, as suggested in Section 3.1. Over seven
302 days, intensities for each magnitude increased gradually accompanying the fact that reference rural
303 temperature also increased from 27.6 °C to 29.2 °C. This reveals that air temperatures in urban areas
304 increase faster than those of the reference rural temperature in this time period, suggesting a typical
305 UHI phenomenon during the summer time. The figure also shows that intensities having a larger m
306 were more stable and with shorter *active* period. For example, the highest peak of the intensities
307 occurred in the mid-night on August 5 when $m = 2$ °C, while the peak was faded when $m = 5$ °C.
308 This suggests that a small m would help to describe the overall evolutionary trend of UHIs while a
309 large one could be able to locate stable heat sources of UHIs.

310 Based on the above statistics, Figure 9 draws UHIs in three magnitudes and presents behaviors
311 of three UHIs queried in the uhi table, with object IDs (the oid column) equalling to 15 ($m=2$ °C),

312 17 ($m=3$ °C), and 10091 ($m=4$ °C). It shows that the UHI having the largest magnitude contracted
 313 insignificantly without any topological transformation and the intensity was stationary throughout
 314 the night. Since this UHI was located in the densest urban area of Guangzhou, it can be formed by
 315 many factors, such as heat exhaust of factories and vehicles, the release of household energy, and heat
 316 storage from building infrastructures, so that they can release the heat continuously and stably at
 317 night-time. Correspondingly, the UHI having a moderate magnitude contracted by separating several
 318 parts from its origin continuously and the intensity decreased gradually. New UHIs occurred from
 319 the separation simultaneously. It can be found that urban temperatures out of the downtown area
 320 decreased faster than that of the reference rural temperature, leading to a decrease of the intensity
 321 and contraction of the zone during the night from 2 am to 4 am. Then, the air started to accumulate
 322 heat at dawn from 5 am to 6 am so that air temperatures increased faster than that of the reference
 323 rural temperature, making expansion and merging. Lastly, UHIs contracted and disappeared when the
 324 sun rises at 7 am because the reference rural temperature has been increased faster and temperature
 325 differences have been smaller than $m=3$ °C. In contrast, the UHI having the smallest magnitude
 326 expanded gradually before dawn but contracted dramatically at dawn, and finally disappeared in the
 327 early morning. The intensity had a contrary evolutionary trend, which decreased and then increased
 328 following by the other decrease during the same corresponding time. It suggests that UHIs in different
 329 magnitudes have different evolutions.

330 Additionally, a UHI can exist throughout several periods (i.e. two active periods are connected
 331 by an inactive period in the `pid` column) as presented in Figure 9. It means that the UHI can either
 332 reappear in the next day (for the UHI with `oid=15`) or in several days (for the UHI with `oid=17`). This
 333 reveals that UHIs have periodicities and demonstrates that the proposed model can track evolutions
 334 of UHIs over a longer time compared with previous models, with the establishing of the periodicity.

335 3.3.2. Thematic evolution of UHIs

336 To find out evolutionary trends of UHIs over seasons, the study investigated into changes of UHIs
 337 in six weeks covering a continuous period of six months from July to December in 2015 (Figure 10).
 338 It shows that UHIs mostly happened and were the most significant at night. However, an entirely
 339 different phenomenon is found that UHIs were the most significant at noon on September 30, October
 340 27 and November 25. This abnormal phenomenon always occurred with a dramatic decrease of the
 341 reference rural temperatures when it was sunny on the previous day and it was raining or cloudy on
 342 the current day. It can be explained that heat accumulated on the previous day could not disperse
 343 immediately at night because of the thermal insulation contributed by the urban canopy, i.e., rain-rich
 344 clouds obstructed the spread of heat. Thus, heat accumulated on the previous day gradually releases
 345 on the next day, and the UHI could become more obviously contributed by anthropogenic heat fluxes
 346 (e.g. heat emission from vehicles) in the daytime.

347 Some findings can also be revealed in Figure 10. UHIs usually occur at night and UHIs with larger
 348 magnitudes are more stable with a shorter active periods. However, intensities at dense urban areas
 349 ($m=4$ °C) can grow dramatically and reach up to 5.5 °C at dawn on September 25 and November
 350 23, making them extremely significant. This phenomenon is always accompanied by clear sky at
 351 night followed by sunshine at dawn. This suggests that continuously clear sky would likely generate
 352 significant UHIs. It can be explained that dense urban areas can release a larger amount of heat
 353 speedily at night with a clear sky so that air temperatures in urban areas can increase much faster
 354 at dawn even though reference rural temperatures increase dramatically. Oppositely, UHIs were
 355 insignificant and even could not happen when amplitudes of the reference rural temperatures became
 356 much smaller between December 20 and December 23, caused by thick fogs all over the days. A similar
 357 phenomenon occurred between August 28 and September 3 that UHIs were short and insignificant

358 over the whole week. However, the mechanism is different, because the heat was dispersed by a
359 rainstorm lasting for the whole week and clouds obstructed absorption of solar radiation fluxes from
360 the land surface. Moreover, continuous raining (e.g. days between August 28 and September 03)
361 and fogs (e.g. days between December 20 and December 23) could obstruct the occurrence of UHIs.
362 Apparently observed from these weathers, daily duration and intensities of UHIs were almost the same
363 from summer to winter, disregarding the seasonal difference.

364 3.3.3. Relationship of UHIs in different magnitudes

365 According to the proposed UHI definition, a UHI in a small magnitude would be more likely to
366 occur within a large zone, so that zones with a large magnitude can locate in the same zone with
367 a small magnitude. Based on the evidence that small and dense urban areas can accumulate great
368 amount of heat from solar heat fluxes (Nichol *et al.*, 2009) and anthropogenic heat fluxes (Zhu *et al.*,
369 2017b), there are reasons to believe that dense urban area could be the largest heat resource in a
370 city. Thus, correlation analysis between areas of zones in the same instant but in different magnitudes
371 would help to explore the relationship of UHIs in different magnitudes.

372 Total areas of UHIs in three magnitudes ($m=2, 3, 4$ °C) were computed through SQL queries
373 and then correlations of the total areas between $m=3, 4$ °C (Figure 11) and between $m=2, 4$ °C
374 (Figure 12) were computed respectively by using R^2 . Overall, $R^2=0.78$ for $m=3, 4$ °C and $R^2=0.59$
375 for $m=2, 4$ °C for six weeks totally. Both cases show positive correlations. These two figures also
376 represent that total area of UHIs were several times (for $m=3$ °C) to dozens of times (for $m=2$ °C)
377 larger those that in a large magnitude ($m=4$ °C).

378 Particularly, all the values of R^2 for $m=3, 4$ °C were larger than 0.80 except for those during
379 seven days between September 25 and October 01 (Figure 11). These values show strong and positive
380 correlations. Two reasons can be discussed. First, dense urban areas determined the evolution of UHIs
381 when $m=4$ °C, since the urban areas and zones of the UHIs had significant overlapping most of the
382 time. Second, a great amount of the heat generated in small and dense urban areas could diffuse to
383 large and low-density urban areas through air thermal diffusion. This process fundamentally affected
384 thermal distribution in low-density urban areas and thus made merging and annexation between zones,
385 as what has been obtained and presented in Figure 9. This reasoning can explain why strong and
386 positive correlations could be shown between areas of zones. Therefore, UHIs in a large magnitude
387 ($m=4$ °C) could overwhelmingly influence evolution of UHIs in a small magnitude ($m=3$ °C).

388 Additionally, the influence could extend across different seasons because $R^2 \geq 0.80$ maintained from
389 August to December basically. It is a weak and positive correlation ($R^2=0.43$) in the period between
390 September 25 and October 01. Given the fact that the weather has been changing a lot during these
391 days, i.e., fogs, clouds, and sunshine were mixed due to different meteorological conditions, it can be
392 deduced that unstable weather can impede heat absorption and thermal diffusion notably, leading to
393 the disappearance of UHIs.

394 Even though all the values of R^2 for $m=2,4$ °C (Figure 12) were smaller than those for $m=3,4$
395 °C (Figure 11), all of them show a positive correlation. Surprisingly, strong and positive correlations
396 remained ($R^2 \geq 0.70$) between July 31 and August 01, October 23 and October 29, and December
397 18 and December 24 for UHIs in $m=2,4$ °C. It can be explained that heat from small and dense
398 urban areas still could influence the evolution of UHIs, spreading into much larger areas in mixed
399 urban-and-rural regions.

400 4. Discussion and conclusion

401 This study established an object-oriented data model organized by graphing in three hierarchies.
402 The model allows tracking of thematic and spatial behaviors of UHIs. Instead of focusing on numeric

403 air temperatures of UHIs, this study proposed the concept of *intensity* as the statistics of temperature
404 differences between urban temperatures and reference rural temperatures to build a model of different
405 behaviors.

406 A UHI has a *magnitude* to maintain its significance and each one may experience several transi-
407 tions between active and inactive periods, which breaks the traditional bondage of tracking UHIs in
408 discrete days and allows a continuous tracking over days, weeks, and even seasons. UHIs at different
409 magnitudes may build inclusive relationships with each other. It means that a large UHI may contain
410 several small UHIs with a large magnitude. As such, the small UHIs would experience active and
411 inactive transitions when the large UHI is active, while the disappearance of the large UHI would lead
412 to the disappearance of all small ones.

413 A simple and effective criterion to test the reliability of the model is set on a concept that each
414 zone has only one behavior at each time instant (no duplicate or undetermined behaviors). The
415 model has been evaluated through a set of input parameters and a complete set of six-weeks data.
416 Several technologies were used in the database management system to accelerate the computation,
417 such as creating indices in spatial and non-spatial columns, tabulating intermediate data maintained
418 in RAMs, and creating a new table to replace an existing one instead of making UPDATE queries.
419 Through these optimizations, computing all the behaviors and establishing all the proposed graphs
420 require about around three minutes.

421 This study has two limitations. First, the spatial density of the stations is not high enough so that
422 micro-changes at the street-block level are difficult to be detected. Second, a UHI undergoes either
423 topological transformation or areal change at each time instant. However, an existing UHI shall have
424 both spatial and thematic properties all the time so that correlations between areas and temperatures
425 for UHIs can be determined continuously. In this consideration, future work can allow a UHI to have
426 areal change and topological transformation at a time instant if the UHI is still active. This study
427 omitted displacements of UHIs as most of them are locationally static. Future work can incorporate
428 this model into other geographical phenomena with obvious displacements, such as water pollutions.
429 Hence, the model has to be improved in a more sophisticated scenario.

430 Four important findings in this study can be summarized, and they suggest the effectiveness of the
431 model. Firstly, clear sky at night connecting sunshine at dawn can promote the occurrence of UHIs
432 of extremely high intensities at dawn. Secondly, UHIs in a specific magnitude could maintain their
433 intensities during the daytime not only in summer but also across winter without the influence of
434 rainy and foggy weather. Thirdly, UHIs normally occur at night across different seasons, while they
435 can also be very significant at noon because of a sunny-to-rainy/cloudy weather in two consecutive
436 days. Lastly, UHIs in a larger magnitude are more readily associated in locations with smaller spatial
437 extents and shorter duration of active periods.

438 To sum up, two conclusions can be drawn. First, the model has four originalities: a new definition
439 for investigating into UHIs in different significances, a new transition between active and inactive
440 periods to extend the life span of UHIs, a new concept of UHI-graph to track dynamics of UHIs,
441 and a new method to compute spatial behaviors confidently. Second, based on a well designed and
442 implemented database management system, the empirical evaluation suggests that the proposed model
443 can process a large set of images and can allow queries to explore evolutions and characteristics of
444 UHIs effectively.

445 **Acknowledgements**

446 This work was supported in part by General Research Fund (project id: 515513) from the Research
447 Grants Council of Hong Kong. The authors also thank the support from National Research Foundation

448 Singapore (NRFS) and Singapore-MIT Alliance for Research and Technology (SMART).

449 **References**

450 Bothwell, J., & Yuan, M. (2010). Apply concepts of fluid kinematics to represent continuous space-time
451 fields in temporal GIS. *Annals of GIS*, 16(1), 27–41.

452 Bothwell, J., & Yuan, M. (2011). A Kinematics-based GIS Methodology to Represent and Analyze
453 Spatiotemporal Patterns of Precipitation Change in IPCC A2 Scenario. *ACM SIGSPATIAL GIS*
454 '11, 152–161.

455 Bothwell, J., & Yuan, M. (2012). A Spatiotemporal GIS Framework Applied to the Analysis of Changes
456 in Temperature Patterns. *Transactions in GIS*, 16(6), 901–919.

457 Buyantuyev, A., & Wu, J. (2010). Urban heat islands and landscape heterogeneity: linking spa-
458 tiotemporal variations in surface temperatures to land-cover and socioeconomic patterns. *Landscape*
459 *Ecology*, 25(1), 17–33.

460 Claramunt C., & Thériault M. (1995). Managing Time in GIS: An Event-Oriented Approach. *Pro-*
461 *ceedings of the International Workshop on Temporal Databases: Recent Advances in Temporal*
462 *Databases*, 23–42.

463 Cohn, E. G., & Rotton, J. (2000). Weather, seasonal trends and property crimes in Minneapolis,
464 1987-1988. A moderator-variable time-series analysis of routine activities. *Journal of Environmental*
465 *Psychology*, 20(3), 257–272.

466 Chai, H. X., Cheng, W. M., Zhou, C. Q., Chen, X., Ma, X. Y., & Zhao, S. M. (2011). Analysis and
467 comparison of spatial interpolation methods for temperature data in Xinjiang Uygur Autonomous
468 Region, China. *Natural Science*, 3(12), 999–1010.

469 Del Mondo, G., Rodríguez, M. A., Claramunt, C., Bravo, L., & Thibaud, R. (2013). Modelling
470 Consistency of Spatio-temporal Graphs, *Data & Knowledge Engineering, Elsevier*, 84(1), 59–80.

471 Ding, Z., Guo, P., Xie, F., & et al. (2015). Impact of diurnal temperature range on mortality in a
472 high plateau area in southwest China: A time series analysis. *Science of the Total Environment*,
473 526, 358–365.

474 Field, S. (1992). The effect of temperature on crime. *British Journal of Criminology*, 32(3), 340–351.

475 Fung, W. Y., Lam, K. S., Hung, W. T., Pang, S. W., & Lee, Y. L. (2006). Impact of urban temperature
476 on energy consumption of Hong Kong. *Energy*, 31(14), 2623–2637.

477 Goodchild M. F., Yuan M., & Cova T. J. (2007). Towards a general theory of geographic representation
478 in GIS. *International Journal of Geographical Information Science*, 21(3), 239–260.

479 Hua, L. and Wang, M., 2012. Temporal and spatial characteristics of urban heat island of an estuary
480 city, China. *Journal of Computers*, 7(12), 3082–3087.

481 Hornsby K., & Egenhofer M. J. (2000). Identity-based change: a foundation for spatio-temporal
482 knowledge representation. *International Journal of Geographical Information Science*, 14(3), 207–
483 224.

484 Hornsby, K. S., & Cole, S. (2007). Modeling Moving Geospatial Objects from an Event-based Per-
485 spective. *Transactions in GIS*, 11(4), 555–573.

- 486 Hofstra, N., Haylock, M., New M., Jones, P., & Frei, C. (2008). Comparison of six methods for
487 the interpolation of daily, European climate data. *Journal of Geographical Research*, 113, D21110.
488 doi:10.1029/2008JD010100
- 489 Hu, L., & Brunsell, N. A. (2015). A new perspective to assess the urban heat island through remotely
490 sensed atmospheric profiles. *Remote Sensing of Environment*, 158, 393–406.
- 491 Irmak, A., Ranade, P. K., Marx, D., Irmak, S., Hubbard, K. G., Meyer, G. E., & Martin, D. L.
492 (2010). Spatial Interpolation of climate variables in Nebraska. *Transactions of the ASABE*, 53(6),
493 1759–1771.
- 494 Jalan, S. and Sharma, K., 2014. Spatio-temporal assessment of land use/land cover dynamics and
495 urban heat island of Jaipur city using satellite data. *The International Archives of the Photogram-*
496 *metry, Remote Sensing and Spatial Information Sciences*, XL(8), 767–772.
- 497 Keramitsoglou, I., Kiranoudis, C. T., Ceriola, G., Weng, Q., & Rajasekar, U. (2011). Identification and
498 analysis of urban surface temperature patterns in Greater Athens, Greece, using MODIS imagery.
499 *Remote Sensing of Environment*, 115(12), 3080–3090.
- 500 Kenney, W. L., Craighead, D. H., & Alexander, L. M. (2014). Heat Waves, Aging, and Human
501 Cardiovascular Health. *Medicine & Science in Sports & Exercise*, 46(10), 1891–1899.
- 502 Kourtidis, K., Georgoulas, A. K., Rapsomanikis, S., Amiridis, V., Keramitsoglou, I., Hooyberghs, H.,
503 Maiheu, B., & Melas, D. (2015). A study of the hourly variability of the urban heat island effect in
504 the Greater Athens Area during summer. *Science of the Total Environment*, 517, 162–177.
- 505 Li, J., Liang, Y., & Wan, J. (2013). Geo-Ontology-Based Object-Oriented Spatiotemporal Data Mod-
506 eling. *Lecture Notes in Computer Science*, 7719, 302–317.
- 507 McIntosh, J., & Yuan, M. (2005). Assessing Similarity of Geographic Processes and Events. *Transac-*
508 *tions in GIS*, 9(2), 223–245.
- 509 Morabito, M., Crisci, A., & Moriondo, M. (2012). Air temperature-related human health outcomes:
510 Current impact and estimations of future risks in Central Italy. *Science of the Total Environment*,
511 441, 28–40.
- 512 Nichol, J. E., Fung, W. Y., Lam K. S., & Wong, M. S. (2009). Urban heat island diagnosis using
513 ASTER satellite images and ‘in situ’ air temperature. *Atmospheric Research*, 94(2), 276–284.
- 514 Nixon, V., & Hornsby, K. S. (2010). Using geolifespans to model dynamic geographic domains. *Inter-*
515 *national Journal of Geographical Information Science*, 24(9), 1289–1308.
- 516 Pultar, E., Cova, T. J., Yuan, M., & Goodchild, M .F. (2010). EDGIS: a dynamic GIS based on space
517 time points. *International Journal of Geographical Information Science*, 24(3), 329–346.
- 518 Papakostas, K., Mavromatis, T., & Kyriakis, N. (2010). Impact of the ambient temperature rise on the
519 energy consumption for heating and cooling in residential buildings of Greece. *Renewable Energy*,
520 35(7), 1376–1379.
- 521 Renolen, A. (2000). Modelling the Real World: Conceptual Modelling in Spatiotemporal Information
522 System Design. *Transactions in GIS*, 4(1), 23–42.
- 523 Rotton, J., & Cohn, E. G. (2004). Outdoor temperature, climate control, and criminal assault. *Envi-*
524 *ronment and Behavior*, 36(2), 276–306.

- 525 Stahl, K., Moore, R. D., Floyer, J. A., Asplin, M. G., & McKendry, I. G. (2006). Comparison of ap-
526 proaches for spatial interpolation of daily air temperature in a large region with complex topography
527 and highly variable station density. *Agricultural and Forest Meteorology*, 139, 224–236.
- 528 Toparlar, Y., Blocken, B., Vos, P., Heijst, G. J. F., Janssen, W. D., Hooff, T., Montazeri, H., &
529 Immermans, H. J. P. (2015). CFD simulation and validation of urban microclimate: A case study
530 for Bergpolder Zuid, Rotterdam. *Building and Environment*, 83, 79–90.
- 531 Wong, M. S., & Nichol, J. E. (2013). Spatial variability of frontal area index and its relationship with
532 urban heat island intensity. *International Journal of Remote Sensing*, 34(3), 885–896.
- 533 Wong, M. S., Zhu, R., Liu, Z., Lu, L., Peng, J., Tang, Z., Lo, C. H., & Chan, W. K. (2016). Estimation
534 of Hong Kong’s solar energy potential using GIS and remote sensing technologies. *Renewable Energy*,
535 99, 325–335.
- 536 Wu, F., Wang, X., Cai, Y., Yang, Z., & Li, C. (2012). Spatiotemporal analysis of temperature-
537 variation patterns under climate change in the upper reach of Mekong River basin. *Science of the*
538 *Total Environment*, 427-428, 208–218.
- 539 Yuan, M., & Hornsby, K. (2008). *Computation and Visualization for Understanding Dynamics in*
540 *Geographic Domains*. CRC Press.
- 541 Yuan, C., & Ng, E. (2012). Building porosity for better urban ventilation in high-density cities - A
542 computational parametric study. *Building and Environment*, 50, 176–189.
- 543 Zhou, B., Kropp, J., & Rybski, D. (2016). Assessing Seasonality in the Surface Urban Heat Island of
544 London. *Journal of Applied Meteorology and Climatology*, 55, 493–505.
- 545 Zhu, R., Guilbert, E., & Wong, M.S. (2017a). Object-oriented tracking of the dynamic behavior of
546 urban heat islands. *International Journal of Geographical Information Science*, 31(2), 405–424.
- 547 Zhu, R., Wong, M. S., Guilbert, E., & Chan, P. W. (2017b). Understanding heat patterns produced
548 by vehicular flows in urban areas. *Scientific Reports*, 7, 16309.

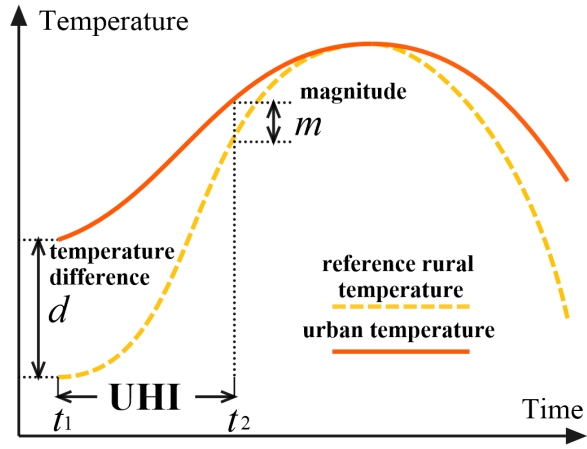


Figure 1: A UHI is with at least m degrees Celsius higher than the reference rural air temperature.

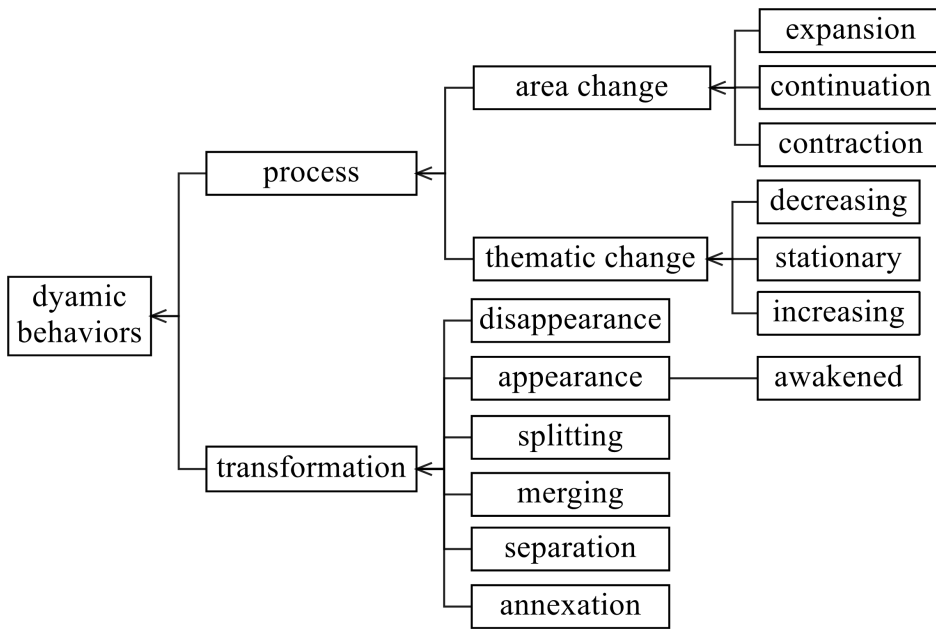


Figure 2: A hierarchical set of dynamic behaviors of UHIs.

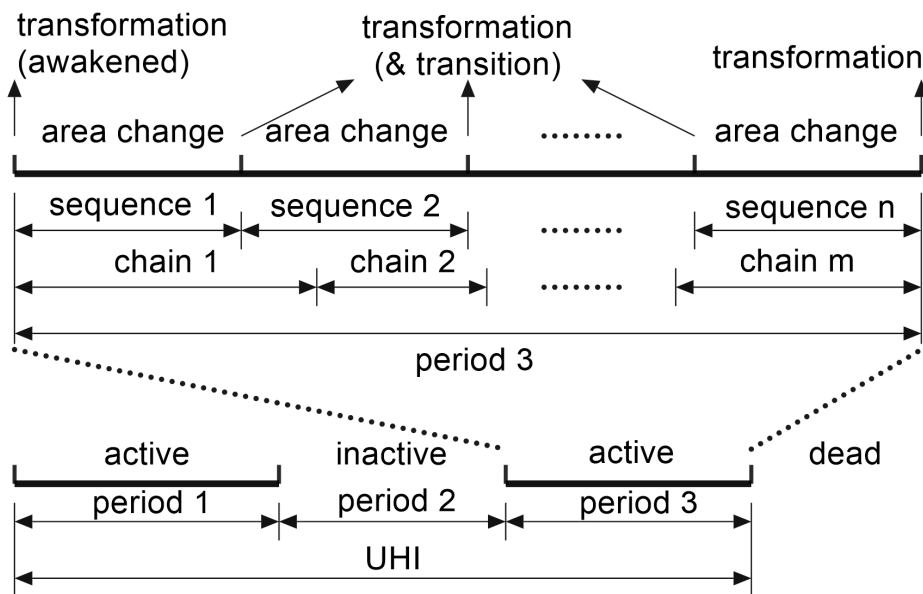


Figure 3: Complete life-cycle of a UHI. An active period contains a series of sequences and chains over a period, in which a sequence is made by a type of spatial behavior associated with transformations and chains correspond to thematic changes.

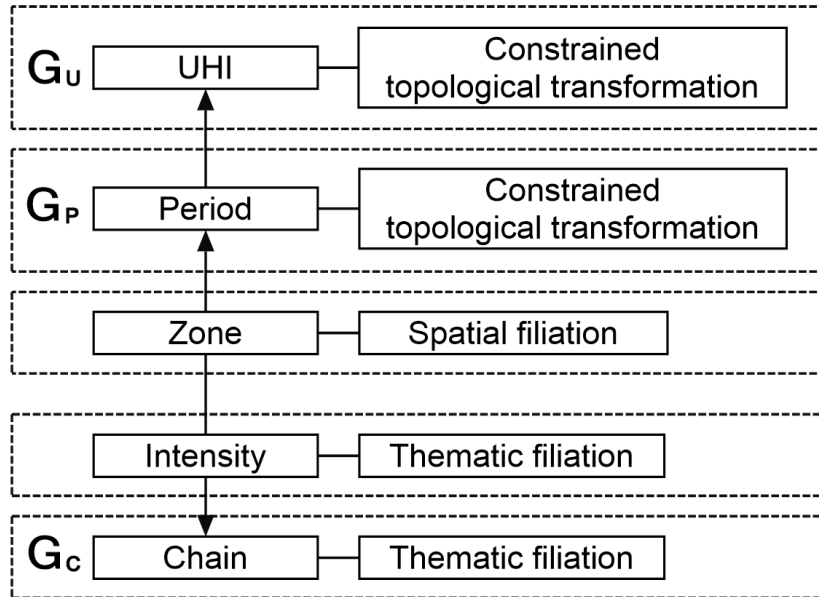


Figure 4: Three hierarchical graphs for UHIs.

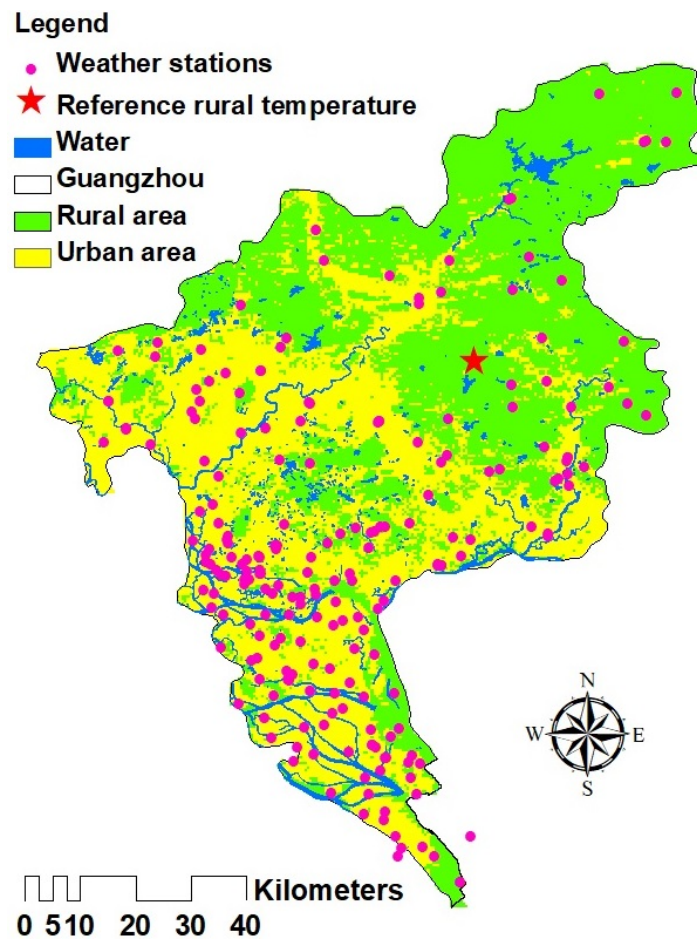


Figure 5: Weather stations are dominantly located in the urban areas of Guangzhou.

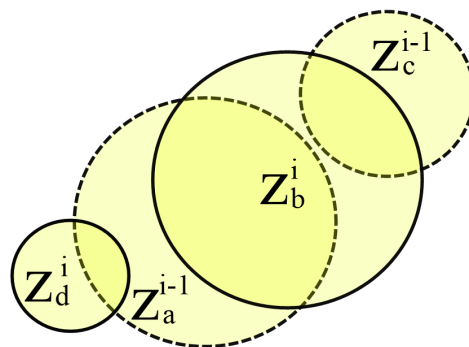


Figure 6: Different overlapping scenarios generate different spatial behaviors.

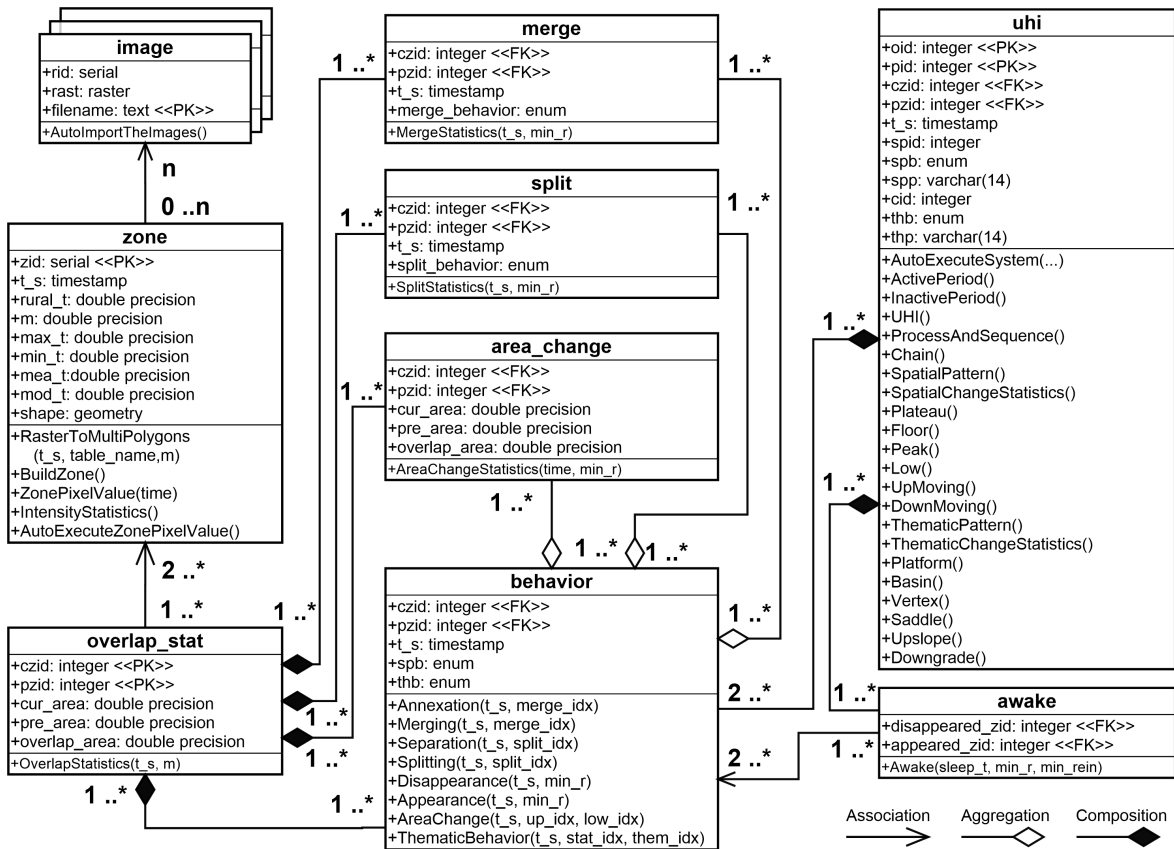


Figure 7: A UML model to present database tables, functions, and their associations and generations for tracking spatial and thematic behaviors of UHIs over time.

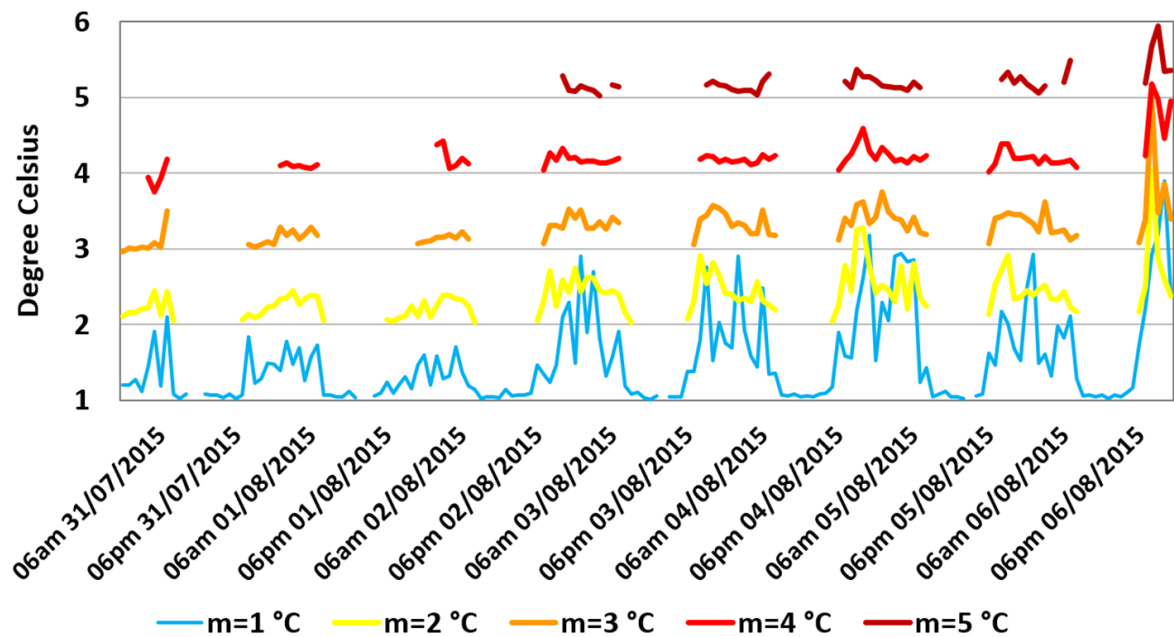


Figure 8: Intensities of UHIs in five different magnitudes for consecutive of seven days.

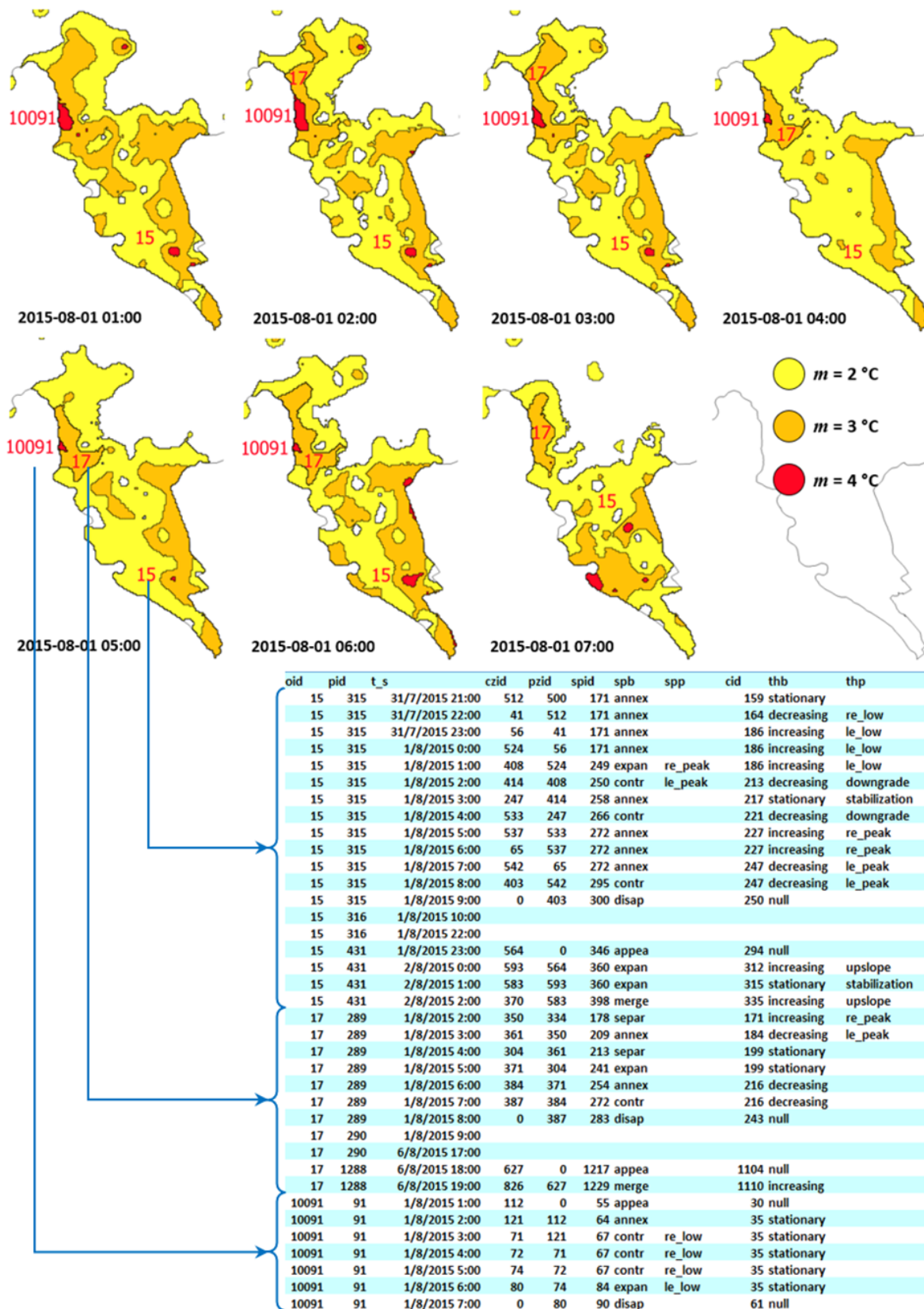


Figure 9: Behaviors of UHIs in three magnitudes of 2, 3, and 4 degrees Celsius.

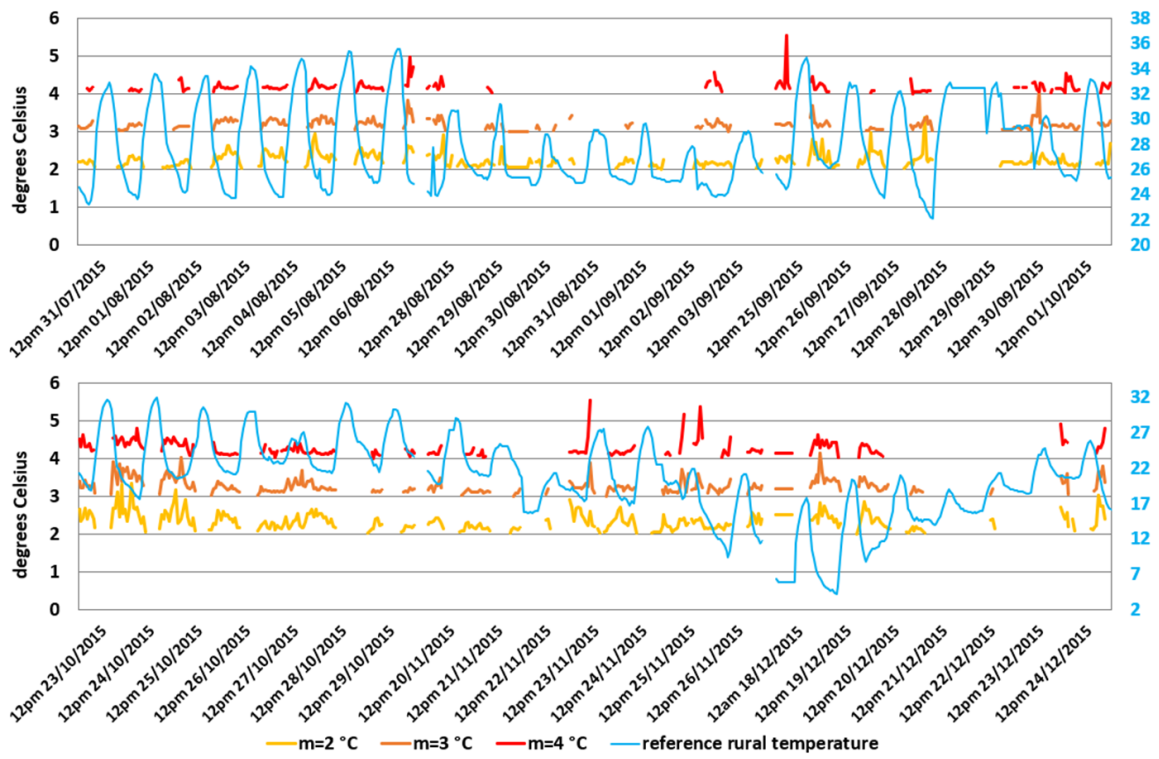


Figure 10: Intensities in three magnitudes over six weeks together with the reference rural temperatures.

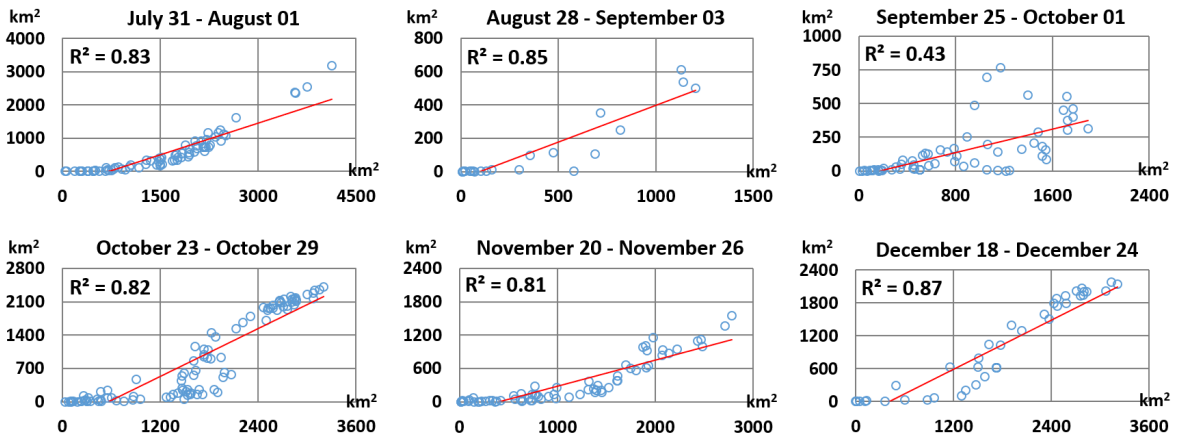


Figure 11: Correlation analysis between areas of UHIs in $m=3\text{ }^{\circ}\text{C}$ (x axis) and $m=4\text{ }^{\circ}\text{C}$ (y axis) over six weeks.

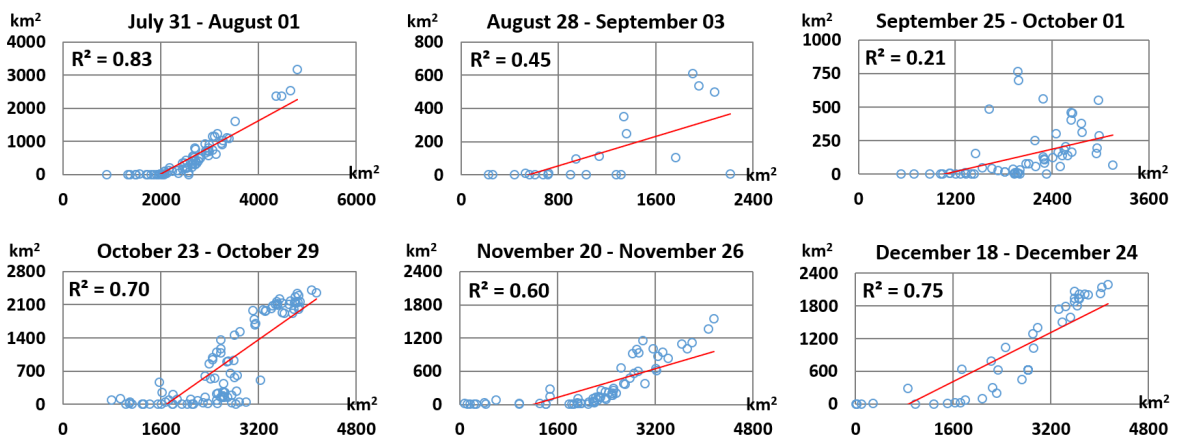


Figure 12: Correlation analysis between areas of UHIs in $m=2\text{ }^{\circ}\text{C}$ (x axis) and $m=4\text{ }^{\circ}\text{C}$ (y axis) over six weeks.